NUCLEAR ENGINEERING AND TECHNOLOGY
ISSN / eISSN 1738-5733
Publisher KOREAN NUCLEAR SOC,
NUTOPIA BLDG, 342-1 JANGDAE-DONG,
DAEJEON, SOUTH KOREA, 305-308,
Volume 26-Issue 1-(2026)
DOI:https://doi.org/10.65281/731888

Effect of Tempering Heat Treatment on Corrosion Behavior of API 5L Grade B Carbon Steel in Albian water

Abdellatif Mamanou [1,*], Helal Yazid [2,3], Fatiha Chelgham [3], Amine Brick Chaouche [4], Brahim Gharbi [1], Salah Eddine Rahmani [5]

[1] Laboratory of Radiation, Plasmas and Surface Physics, University of Kasdi Merbah Ouargla, 30000 (Algeria).

[2] LMSM, Mechanical Engineering Department, University of Biskra, B.P. 145, 07000, Biskra (Algeria).

[3] Department of Drilling and Mechanics of Oil Fields, University Kasdi Merbah Ouargla, 30000 (Algeria).

[4] Research Center in Industrial Technologies (CRTI), P.O.Box 64, 16014, Cheraga, Algiers (Algeria).

[5] Laboratory for Inorganic, Organic, and Bio-Inspired Chemistry Research, University of Djelfa, 17000 (Algeria).

[*] Corresponding author: mamanou.abdellatif@univ-ouargla.dz

Received : 21/12/2025 ; Accepted : 23/04/2026

Abstract

The effect of tempering on the corrosion behavior of API 5L Grade B carbon steel in Albian water was investigated in this study. Carbon steel samples were tempered at 200 °C, 300 °C, 400 °C, and 500 °C for one hour and analyzed using X-ray diffraction (XRD), XRF, optical microscopy, Vickers microhardness tests, and potentiodynamic measurements. Chemical analysis showed that Albian water was rich in corrosive ions, mainly chloride and sulfate. Metallographic examination of the as-received steel revealed a microstructure composed of ferrite and pearlite phases. The electrochemical potential difference between these phases generates local microgalvanic cells in the corrosive medium, leading to anodic dissolution of cementite lamellae in pearlite. The XRD analysis showed tensile residual stresses within the microstructure. Results showed that as the tempering temperature increased, the microhardness and corrosion rate of the carbon steel gradually decreased due to reduced dislocation density, residual stress relief, and carbide redistribution. According to the Tafel polarization curve method, the corrosion rates for tempered samples at 200, 300, 400, and 500°C for 1 hour were 0.157, 0.113, 0.095, and 0.055 mm/yr, respectively.

Keywords: corrosion, API 5L Grade B, carbon steel, Albian water, tempering, heat treatments, microhardness, ferrite, pearlite.

1. Introduction

Pipelines are widely used in the petroleum industry to efficiently transport crude oil and natural gas over long distances, from extraction sites to processing, storage, or refining facilities, ensuring a continuous, efficient, and cost-effective flow of energy resources.[1] [2]

Moreover, pipelines play a central role in water injection (WI), the most cost-effective enhanced oil recovery (EOR) method for maintaining stable production rates, especially in near-depletion wells. This method involves pumping pressurized water into the reservoir through injection wells to push residual crude oil or gas within the formation's pores toward production wells. Water injection pipelines (WIPs) connect surface facilities, such as water treatment plants, pumping stations, and storage tanks, to the injection wells. [3]

WIPs are primarily made of carbon steel because it offers cost-effectiveness and appropriate mechanical properties, such as strength, durability, weldability, and sufficient corrosion resistance. The injected water is selected based on economic factors such as pipeline location and water resource availability.

However, due to continuous exposure of WIPs to injected water rich in highly corrosive species, the integrity of carbon-steel pipelines could be seriously compromised. This leads to severe corrosion problems and can result in significant economic losses due to unplanned workovers and the cost of replacing failed equipment.

Considering the damage caused by this issue, assessing the corrosion of metallic equipment used in various petroleum environments is essential for developing effective methods to prevent and manage corrosion damage [4] [5]

In the oil and gas industry, several techniques are commonly employed to control corrosion, such as adding chemical corrosion inhibitors to corrosive media, implementing cathodic protection, applying organic coatings to the material's surface, and subjecting the material to heat treatment. All these methods focus on one of the following strategies: altering the properties of the corrosive medium, creating a barrier between the material and its environment, or enhancing the material's resistance against corrosion. [5]

Corrosion inhibitors are often added to environments to prevent the failure of carbon steel pipe. Chemical or electrochemical reactions between inhibitors and the environment form a protective thin film on the metal surface. Inhibitors can also alter the properties of the corrosive medium, making it less aggressive and thus protecting the metal. However, as the temperature rises or the inhibitor concentration decreases, the inhibitor's effectiveness declines. In the water injection recovery process, water is injected at high pressure and high temperature into the pipeline, which compromises the formation of a protective layer on carbon steel in water injection systems.

The corrosion behavior and mechanical properties of metals and alloys can be enhanced through heat treatments, which consist of precise heating and cooling of the metal over time. Among heat treatments, tempering is widely used to reduce residual stress, increase fracture resistance, and improve corrosion behavior. In this process, the metal is heated to a temperature below its critical point for a precise period, then cooled, typically in air.[6] [7]

Many researchers have investigated the influence of heat treatment on the corrosion behavior of carbon steel. The contents concluded that the steel composition, heat treatment conditions, and the characteristics of the corrosive environment all significantly influence corrosion.[8] [9]

HM Lieth et al. (2021) examined API 5L X60 steel after austenitizing at 800 °C or 900 °C, followed by tempering at 300 °C, 450 °C, or 600 °C, then immersion in crude oil, seawater, or freshwater for 42 days. Corrosion was measured by weight loss, and microstructure, microhardness, and impact toughness were also evaluated. They reported that the best corrosion resistance in freshwater and seawater was achieved with 900 °C austenitizing plus 300 °C tempering, yielding about a 63% reduction in freshwater and 60% in seawater relative to untreated steel. In crude oil, the response was weaker; the best result was about a 22% reduction, obtained at 800 °C austenitizing plus 300 °C tempering. The untreated specimens corroded more in seawater than in freshwater, and least in crude oil. [10]

A. Wojtacha examined the impact of thermal treatment on the corrosion of high-strength HSLA steel, which was exposed for 16 days to continuous spraying of selected solutions. The results from the gravimetric method and potentiometric tests showed that the martensite microstructure subjected to tempering heat treatment exhibited the highest corrosion resistance. Moreover, the corrosion rate of steel was significantly influenced by the acidity of the corrosion environment. It was reported that the best corrosion behavior was observed in NaOH solution, and the worst in H_2SO_4 solution. The tested alloy showed excellent corrosion resistance in a 3.5% NaCl solution, which simulates artificial seawater; therefore, the studied steel can be used in offshore drilling and petroleum production. [11]

Lochan Sharma and Rahul Chhibber investigated how heat treatment alters the microstructure of API X70 linepipe steel and consequently influences its corrosion resistance and mechanical properties. They applied to the steel a process of Austenization, followed by quenching and tempering at 300°C, 450°C, and 600°C, then exposed the specimens for 30 days to four environments (fresh water (pH 7), seawater (pH 8.2), and acidic NaCl solutions at pH 3 and 5). Their key finding was that higher tempering temperatures produced ferritic microstructures with significantly lower corrosion rates, while lower temperatures retained tempered martensite with higher hardness but greater corrosion susceptibility. This demonstrates that heat treatment temperature critically balances the trade-off between strength and corrosion resistance for pipeline applications in aggressive service environments. Moreover, they have concluded that the corrosion resistance of the examined steel is also influenced by pH and the concentrations of the exposure solutions. [4]

S. Hakan Atapeka et al. (2012) explored the corrosion behavior of low-carbon steel exposed to different heat treatment processes, including Austenitizing at 1000°C for 30 minutes, water quenching, and tempering at temperatures between 200 and 600°C. Their results revealed that the corrosion rate of the carbon steel in 3.5% NaCl was evaluated by weight loss after immersion tests for up to 7 days and confirmed by potentiodynamic polarization. They concluded that the corrosion behavior of the carbon steel was affected by the tempering temperature, the hardness, and the resulting microstructure. [9]

The present study aims to investigate the influence of tempering heat treatment on the corrosion behavior of API 5L Grade B carbon steel pipelines used to inject Albian water in Haoud Barkaoui Oilfield (located in southern Algeria). To achieve this goal, samples of carbon steel were tempered at various temperatures, 200, 300, 400, and 500 °C, for 1 hour, then examined using optical microscopy, XRD, XRF, Vickers microhardness test, and electrochemical methods for exploring the variation in microstructure and measuring the corrosion rate of the tested steel upon tempering temperature.

2. Materials and methods

Experiments were conducted using API 5L Grade B carbon steel, as-received, from water-injection pipelines at the Haoud Barkaoui oilfield.

The chemical composition of the carbon steel sample was analyzed using a Bruker S1 TITAN Handheld XRF Analyzer. The corrosive media used in this research consisted of Albian water collected from wells in the Haoud Berkaoui oilfield.

API 5L Grade B carbon steel pipe samples were prepared as follows. After cutting the samples into various shapes and dimensions, their surfaces were abraded with SiC abrasive paper ranging from 220# to 1250# to achieve a mirror-like finish. The samples were then cleaned with acetone for 15 minutes to remove residual impurities, followed by air drying. They were then immersed in ethanol for 5 minutes, washed in distilled water, and finally dried for 5 minutes.

Metallographic examination was used to evaluate the nature of the carbon steel microstructure and its effect on the corrosion mechanism. Firstly, the polished as-received sample's surface was etched in 2% Nital solution for 10 seconds at room temperature, then examined using the "EUROMEX MIC 3678" optical microscope.

The as-received and tempered carbon steel samples were examined by X-ray diffraction (XRD) using a Bruker D2 PHASER diffractometer run at 40 kV and 30 mA with Co-Kα radiation $\left(\lambda_{Co} = 1.7887\text{Å}\right)$. The scan reflection angle range was from 20° to 120°, with a step width of 0.02°. The obtained XRD patterns were further analyzed to identify the crystalline properties of the sample and to determine the influence of tempering on microstructure and the corrosion behavior of the tested carbon steel.

Vickers microhardness measurements of as-received and tempered samples were performed using a Future-Tech FM-300e microhardness tester. A 0.1 kg load was used for the tests.

Potentiodynamic polarization measurements were conducted on API 5L Grade B carbon steel samples in Albian water at room temperature. A Potentiostat/Galvanostat Voltalab PGP201 model, controlled by Volta Master 4.0 software, was used to perform the corrosion tests, along with a glass corrosion cell that includes a platinum auxiliary electrode, a Saturated Calomel reference electrode, and working electrodes made of tempered carbon steel samples. The applied polarization potential ranged from -800 mV to -350 mV, with a scan rate of 25 mV/minute.

3. Results and discussions

3.1 Material and solution analysis

The XRF analysis of the studied carbon steel and the API 5L Grade B Standard are shown in Table 1. The chemical composition and pH value of the Albian water sample are shown in Table 2.

Table 1. Chemical composition of API 5L grade B carbon steel.

Elements	Content (wt%)	API 5L Grade B Standard
C	0.2200	0.26 max
Si	0.1200	
S	0.0300	0.030 max
P	0.0300	0.030 max
Mn	0.9600	1.2 max
Ni	0.1000	0.5 max
Cr	0.1000	0.5 max
Mo	0.0300	0.15 max
Cu	0.0800	0.5 max
Ti	0.0008	Nb + V + Ti < 0.15
Nb	0.0005	V + Nb < 0.06
V	0.0050	V + Nb < 0.06
Fe	Balance	

Chemical analysis confirms that the carbon steel composition meets the requirements of API 5L Grade B. Additionally, since the sample's carbon content is less than 0.30%, it qualifies as low-carbon steel.

Samples of Albian water were collected from the Haoud Berkaoui oil field and analyzed for composition and pH. The results are summarized in Table 2.

Table 2: The chemical composition of Albian water collected from the Haoud Berkaoui oilfield

Ion	Ca^{+2}	Mg^{+2}	Na^{+}	K^{+}	Cl^{-}	$SO4^{-2}$	$HCO3^{-}$	$NO3^{-}$	pH
(mg/l)	197	142.1	365	55	500	1107	189	1.3	7.79

Table 2 shows a pH value greater than 7, confirming the slightly alkaline nature of Albian water. The predominant anions in this water were Cl^- and SO_4^{2-}, while the most prevalent cations were Na^+, K^+, Ca^{+2}, and Ba^{+2}.

Previous studies have shown that chloride (Cl^-) and sulfate (SO_4^{2-}) ions promote corrosion of carbon steel through various mechanisms. [12]

Multi-phase carbon steels are particularly vulnerable to localized corrosion in chloride-rich solutions. Moreover, due to its high electronegativity and solubility, chloride can penetrate and disintegrate the passive films formed by oxides or other corrosion products that normally protect carbon steel surfaces, exposing the metal directly to the corrosive environment and accelerating the redox reaction, thereby intensifying the carbon steel dissolution. Furthermore, Cl^- can increase water conductivity, which increases the corrosion rate of carbon steel.[13]

On the other hand, in slightly alkaline solutions, SO_4^{2-} ion accelerates iron oxidation by forming soluble complexes with Fe^{+2} and Fe^{+3}. Furthermore, iron is highly soluble in sulfate solutions, creating a supersaturated solution that permits the precipitation of a non-protective layer. [14]

3.2 Metallographic examination

The microstructure of the as-received carbon steel sample is shown in Figure 1. It consists of two phases: ferrite (α-Fe) and pearlite (p), which appear as dark and light shades, respectively. Pearlite is a dual-phase microstructure composed of ferrite and cementite. [15]

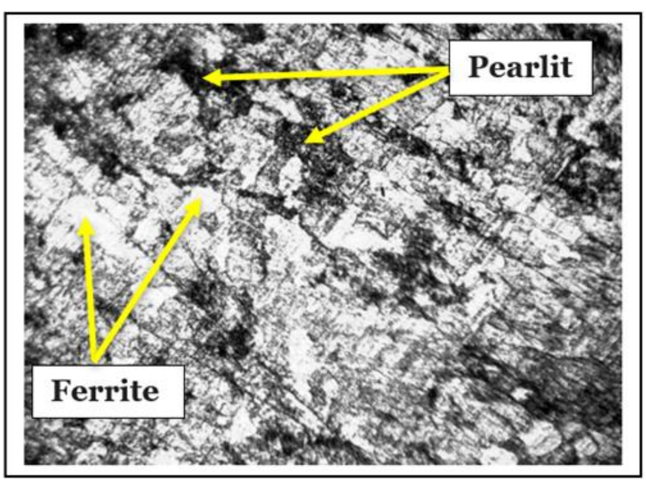

Fig1. Microstructure of API 5L Grade B steel sample etched with 2% natal (ferrite–pearlite two-phase microstructure). 50x

This result is consistent with previous investigations, which confirm that low-carbon steels typically possess a microstructure composed of ferrite and pearlite.[14] [15]

3.3 X-ray diffraction

XRD patterns of the API 5L carbon steel sample, tempered at 200, 300, 400, and 500 °C, for 1 h, are illustrated in Fig.2. The obtained XRD spectra were further analyzed to determine the influence of tempering on microstructure and other crystalline properties correlated to the corrosion resistance of the tested carbon steel.

The XRD patterns were all similar; they exhibited three visible diffraction peaks at 52.757°, 77.482°, and 99.916°, corresponding to the (110), (200), and (211) reflections of the ferrite phase (α-Fe). However, the diffraction peaks of cementite and other carbide phases were not detected because of their low proportions in the matrix. Typically, carbide phases must be present at around 5% or more by volume to produce sufficiently strong diffraction peaks detectable by XRD.

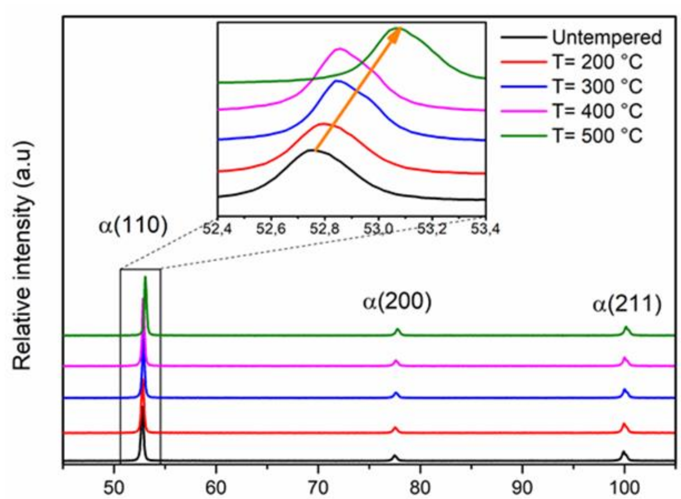

Fig.2: A combined XRD pattern of the studied steel tempered at different temperatures, with the inset showing a zoom-in view of the shift in the (110) plane of the steel samples.

As seen in Figure 2, by increasing tempering temperature, XRD peaks shift slightly towards higher 2θ angles, indicating a contraction in lattice interplanar spacing (d-spacing) according to Bragg's law, which describes the relationship between the lattice spacing of a crystal (d), X-ray wavelength (λ), and diffraction angle presented by the equation (1):

$$n\lambda = 2d \sin\theta \quad (1)$$

Where: n is an integer denoting the diffraction order. By differentiating Bragg's equation,

$$\Delta\theta = -(\Delta d/d) tan\theta \quad (2)$$

Where Δd represents the change in the lattice spacing of the crystal planes, and $\Delta\theta$ is the X-ray diffraction angle.

From equation (2), it can be seen that any alteration in the lattice spacing of crystal planes will result in a variation in the X-ray diffraction angle.

Peak shifting is most likely due to the relief of internal residual stress developed during the previous manufacturing processes and heat treatments of the carbon steel. Tensile stresses introduced at the surface after quenching increase the lattice spacing, thereby shifting the XRD diffraction peaks towards lower angles. In contrast, tempering relief tensile stress and causes contraction in d-space, which shifts the peaks to higher diffraction angles.

In corrosive environments, such as chloride-rich water, tensile stress promotes the initiation of stress corrosion cracks.

3.4 Effect of tempering on grain size and dislocation density

The average grain sizes and dislocation densities of as-received and tempered carbon steel samples were calculated from XRD patterns using the Debye–Scherrer equation (3) and the Stokes–Wilson equation (4), respectively.

$$D = K\lambda/Bcos\theta \quad (3)$$

Here, D, λ, and θ represent the average grain size, the wavelength of the characteristic X-ray, and the diffraction angle, respectively. K is a constant, and B is the full width at half maximum (FWHM) of the peak.[16] [17]

$$\delta = D^{-2} \quad (4)$$

The average crystal grain size as a function of tempering temperature is shown in Figure 3. It is worth noting that the higher the tempering temperature, the larger the grain size. This is consistent with the literature. However, tempering usually has little direct effect on the original grain size because tempering is a subcritical heat treatment: it is done below the austenite transformation range, so it does not create new austenite grains or drive major grain-boundary movement. [18] [19]. The results showed that tempering the steel at 500 °C changed the original grain size from 275 to 289 Å, or by about 14 Å.

As the tempering temperature rises, the thermal activation of dislocations increases, leading to the movement of many dislocations. Some dispersed dislocations within the matrix attract and cancel each other, while others tend to move toward and gather at grain boundaries.

The grain size of the tempered samples as a function of tempering temperature is shown in Figure 3. Tempering reduces dislocation density and internal stresses, which enhances corrosion resistance in carbon steel.

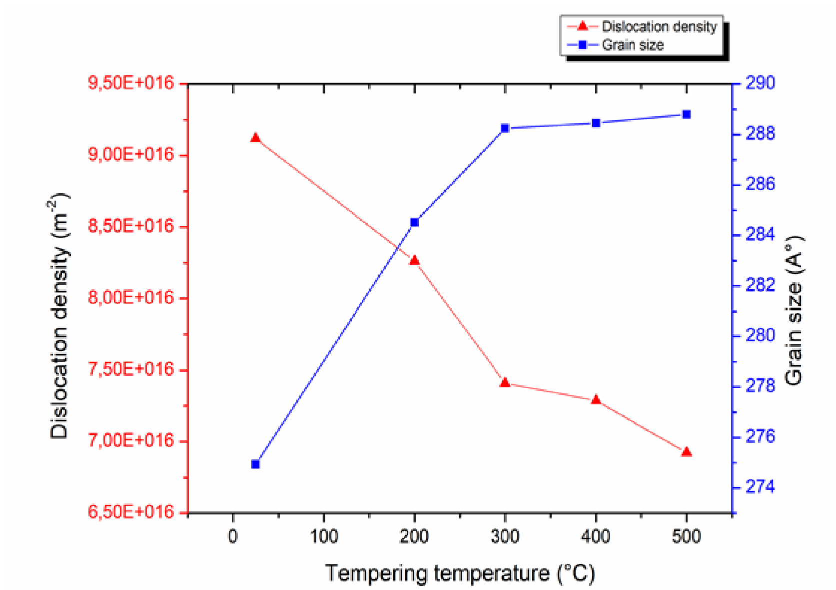

Fig.3 : Grain size and dislocation density vs tempering temperature

3.5 Microhardness

Figure 4 shows the Vickers indentation impression on the sample surface. The average values of measurements taken at random locations on the surface of each API 5L Grade B sample are listed in Table 3 and presented in Figure 5.

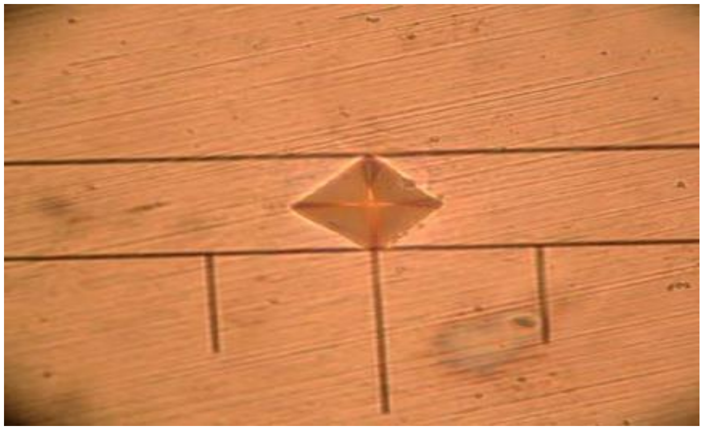

Fig.4 : Metallographic Vickers indentation image

Table 3: Vickers micro-hardness of carbon steel as a function of tempering temperature.

Temperature °C	AR	200	300	400	500
Microhardness	233.1	219.5	202.566	200.94	200

The microhardness of the as-received carbon steel (233.1 HV) is below the maximum allowed by the API standard for oil and gas industry pipelines, which must not exceed 248 HV. Therefore, the carbon steel achieves the requirements of the API Standards. [20]

The variation of micro-hardness versus tempering temperature is shown in Figure 5. The steel's hardness is sensitive to tempering heat treatment. It decreases gradually as the tempering temperature increases. During the pipe manufacturing process, significant internal stresses are introduced into the carbon steel, resulting in a hard, brittle microstructure.

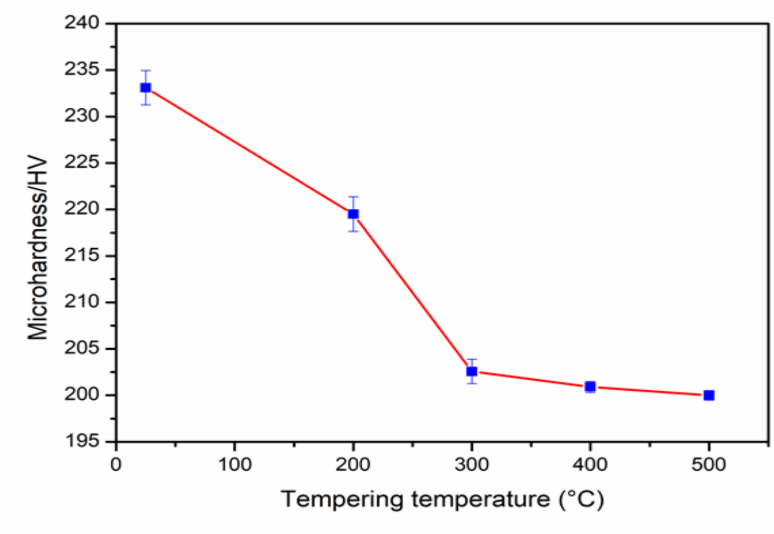

Fig. 5: The effect of tempering temperature on microhardness of API 5L grade B steel

Tempering significantly softens carbon steel by relieving residual stresses, decreasing dislocation density, and carbide coarsening in the microstructure. The microhardness of tempered samples has been compared with that of as-received steel. Notably, the decrease in hardness is more pronounced at higher tempering temperatures. 300-500 °C. The heat-treated carbon steel lost approximately 14.20% of its hardness after being tempered at 500 °C for 1 hour.

3.6 Electrochemical tests

Electrochemical parameters, such as corrosion current density (I_{cor}), corrosion potential (E_{cor}), and corrosion rate (CR), were evaluated using the Tafel method. The obtained results are listed in Table 4. Polarization curves for untreated and tempered carbon steel samples are depicted in Figure 6.

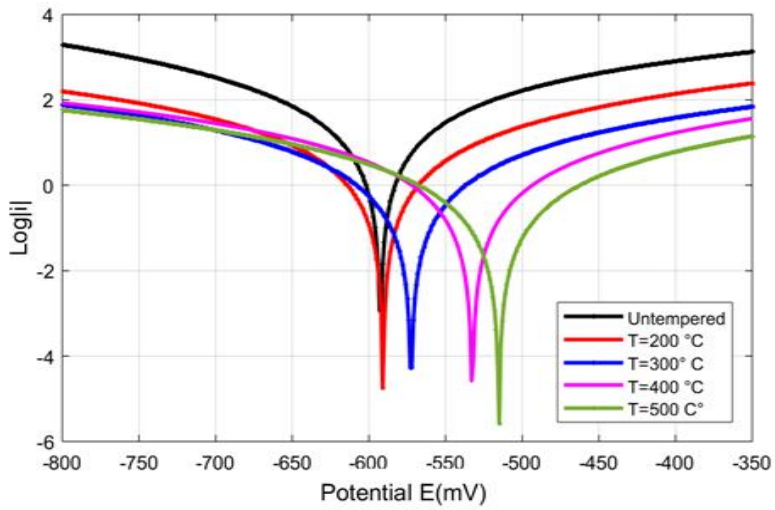

Fig.6: Potentiodynamic polarization curves of as-received and tempered samples

Table 4. Electrochemical parameters of as-received and tempered API 5L Grade B steels in Albian water

From Figure 6, it can be observed that all curves have similar shapes. However, as the tempering temperature increases, the curves shift slightly toward lower current densities and higher potential zones, indicating a decrease in metal dissolution kinetics. The variation of carbon steel corrosion rate with tempering temperature is represented in Figure 7. The corrosion rate decreases with increasing tempering temperature. [21] [15].

T (C°)	$I_{cor}(\mu A/cm^2)$	$E_{cor}\ (mV)$	$-\beta_c(mV)$	$\beta_a(mV)$	CR (mm/yr)
As received	19.610	-592.5	126.6	226.1	0.229
200	13.4281	-590.8	287.8	255	0.157
300	9.620	-572.5	287.3	308.0	0.113
400	8.091	-532.6	289.1	264.7	0.095
500	4.731	-515.2	207.9	223.6	0.055

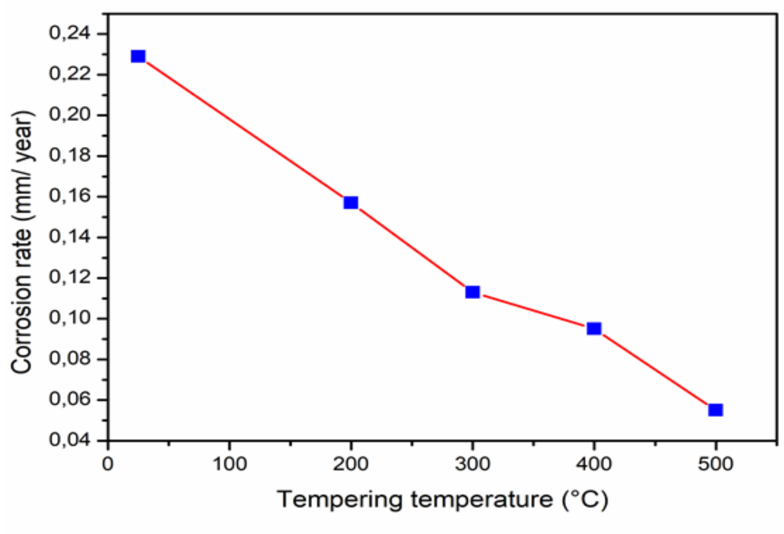

Fig. 7: Corrosion rate of API 5L grade B carbon steel as a function of tempering temperature

Because the sample has a heterogeneous ferrite-pearlite microstructure, differences in electrochemical potential between ferrite and cementite within the pearlite phases form microgalvanic cells when exposed to corrosive media. As the corrosion potential of cementite is greater than that of ferrite, cementite acts as a local cathode, while ferrite acts as a local anode. This results in the selective dissolution of ferrite, which significantly accelerates galvanic corrosion of the steel.

Tempering alters the carbon steel's ferrite-pearlite microstructure by changing the size, distribution, and morphology of cementite particles embedded in the ferrite matrix. As the tempering temperature increases, cementite particles become coarser, more stable, and less uniformly distributed within the ferrite. This reduces the ferrite-cementite interfacial area, thereby lowering galvanic coupling effects and reducing the carbon steel corrosion rate.

On the other hand, the corrosion rate of carbon steels decreases with increasing tempering temperature due to the diminution in dislocation density and the relief of residual stresses. The effect is more significant if the steel is tempered for a long holding time and at higher temperatures. [21]

Figure 8 showed that tempering of API 5L carbon steel for 1 hour at 200°C, 300°C, 400°C, and 500°C reduced the corrosion rate in Albian water by 31.44%, 50.65%, 58.51%, and 75.98%, respectively.

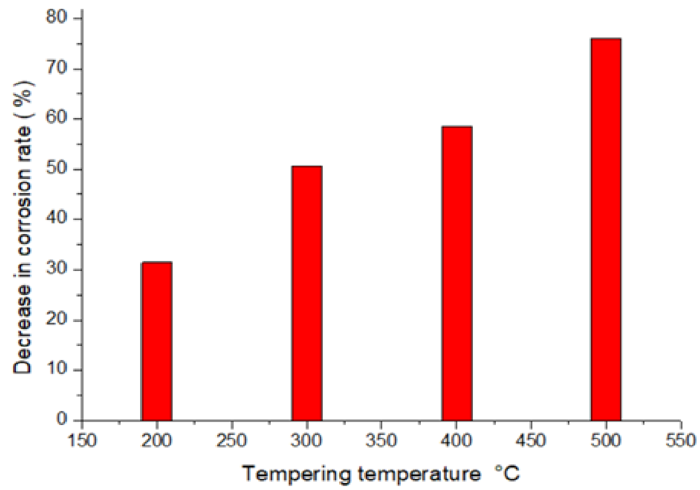

Fig. 8: Decrease in corrosion rate as a function of tempering temperature

4. Conclusion

The effect of tempering heat treatment on the corrosion behavior of API 5L grade B pipeline steel in Albian water was studied in this paper. First, the corrosion environment, consisting of water used in enhanced oil recovery (EOR), and the chemical composition of the carbon steel were analyzed. Then, the steel samples were tempered at 200, 300, 400, and 500 °C for 1 h, and their corrosion rates in the Albian water were measured. According to the obtained results, it can be concluded that:

- The Albian water pH is slightly basic, and its chemical composition shows a high concentration of aggressive ions such as Cl^-, and SO_4^{2-}.
- The API 5L Grade B carbon pipe steel presented a microstructure consisting of ferrite and pearlite. This is typical for low-carbon steels.
- The structural difference between cementite and ferrite phases created micro-galvanic couples in a corrosive medium and led to galvanic corrosion in the steel. The high concentration of chloride ions in injection water accelerates the corrosion in grain boundaries.
- The hardness of the as-received steel (233.1 HV) was found to be less than the maximum value allowed by the API standard of pipe steel used for the oil and gas industry, which must not exceed 248 HV.
- The steel hardness decreases gradually as the tempering temperature increases
- The tempered API 5L Grade B carbon pipe steel at 500 °C, has the lowest Vickers hardness of 200 HV

- The tempering softens the steel and enhances its corrosion resistance, due to a reduction in dislocation density, relief of residual internal stresses, and the alteration in size and density of carbide within the steel microstructure.
- Tempering of the carbon steel for 1 hour at 200°C, 300°C, 400°C, and 500°C reduces the corrosion rate in Albian water by 31.44%, 50.65%, 58.51%, and 75.98%, respectively.

Author Contributions:

Supervision, writing–original draft of the manuscript, tempering heat treatments, and Electrochemical tests, A. Mamanou; Albian Water analysis, Microhardness tests, review and editing, F. Chelgham; XRD and XRF analysis, Y. Helal, A. B. Chaouche, B. Gharbi; samples preparation and Metallographic examination, S.E. Rahmani.

All authors have read this version of the manuscript and agreed to publish it.

Funding:

This research received no external funding

Acknowledgments:

The authors would like to thank the Laboratory of Radiation, Plasma, and Surface Physics, Kasdi Merbah Ouargla University (Algeria), which made this research possible, and Algeria's national oil and gas company (SONATRACH) in Houad Barkoaui Oilfield, for the contribution to this work by providing Albian water and API 5L Grade B pipe samples

Conflicts of Interest:

The authors declare no conflict of interest.

References

[1] K. Tamalmani et H. Husin, « Review on Corrosion Inhibitors for Oil and Gas Corrosion Issues », *Appl. Sci.*, vol. 10, nº 10, p. 3389, mai 2020, doi: 10.3390/app10103389.

[2] H. M. Lieth, R. Al-Sabur, R. J. Jassim, et A. Alsahlani, « Enhancement of corrosion resistance and mechanical properties of API 5L X60 steel by heat treatments in different environments », *J. Eng. Res.*, vol. 9, nº 4B, 2021.

[3] C. Tan *et al.*, « Research on the Damage Mechanism of Oilfield Water Injection System Based on Multiple Operating Conditions », *Processes*, vol. 13, nº 6, p. 1798, juin 2025, doi: 10.3390/pr13061798.

[4] L. Sharma et R. Chhibber, « Effect of Heat Treatment on Mechanical Properties and Corrosion Behaviour of API X70 Linepipe Steel in Different Environments », *Trans. Indian Inst. Met.*, vol. 72, nº 1, p. 93-110, janv. 2019, doi: 10.1007/s12666-018-1465-y.

[5] Y. Dong, « Analysis on anti-corrosion and anti-scaling technology of water injection well in oil production plant », *IOP Conf. Ser. Earth Environ. Sci.*, vol. 514, nº 2, p. 022005, mai 2020, doi: 10.1088/1755-1315/514/2/022005.

[6] O. Olaseinde, D. Folorunsho, et O. Olaniran, « Heat Treatment and Corrosion Behaviour of Selected Steels in 3.5 M Sodium Chloride », *Am. J. Eng. Res. AJER*, vol. 5, nº 5, p. 231-237, 2016.

[7] M. K. Banerjee, « 2.1 Fundamentals of Heat Treating Metals and Alloys », in *Comprehensive Materials Finishing*, Elsevier, 2017, p. 1-49. doi: 10.1016/B978-0-12-803581-8.09185-2.

[8] O. Sunday Isaac Fayomi et A. Patricia Idowu Popoola, « Corrosion propagation challenges of mild steel in industrial operations and response to problem definition », *J. Phys. Conf. Ser.*, vol. 1378, nº 2, p. 022006, déc. 2019, doi: 10.1088/1742-6596/1378/2/022006.

[9] Ş. H. Atapek, Ş. Polat, et S. Zor, « Effect of tempering temperature and microstructure on the corrosion behavior of a tempered steel », *Prot. Met. Phys. Chem. Surf.*, vol. 49, nº 2, p. 240-246, mars 2013, doi: 10.1134/S2070205113020111.

[10] H. M. Lieth, R. Al-Sabur, R. J. Jassim, et A. Alsahlani, « Enhancement of corrosion resistance and mechanical properties of API 5L X60 steel by heat treatments in different environments », *J. Eng. Res.*, vol. 9, nº 4, p. 428-442, déc. 2021, doi: 10.36909/jer.14591.

[11] A. Wojtacha, M. Kciuk, et M. Opiela, « Effect of Heat Treatment Conditions on Corrosion Resistance of 0.28C–1.4Mn–0.3Si–0.26Cr Steel with Nb, Ti, and V Microadditions », *Materials*, vol. 14, nº 12, p. 3254, juin 2021, doi: 10.3390/ma14123254.

[12] N. V. Likhanova *et al.*, « Corrosion Evaluation of Pipeline Steel API 5L X52 in partially deaerated Produced Water with High Chloride Content », *Int. J. Electrochem. Sci.*, vol. 13, nº 8, p. 7949-7967, août 2018, doi: 10.20964/2018.08.13.

[13] M. Y. M. Sholihin, H. S. Kusyanto, et B. Soegijono, « Analysis of the remaining life of API 5L grade B gas pipeline in the flare gas recovery unit », *IOP Conf. Ser. Mater. Sci. Eng.*, vol. 432, p. 012016, nov. 2018, doi: 10.1088/1757-899X/432/1/012016.

[14] V. S. Hadi, F. Mubarok, et M. Fitrullah, « Toughness Recovery of Welded Pipe API 5L Grade B through Quenching and Tempering Treatment », *Key Eng. Mater.*, vol. 939, p. 19-24, 2023.

[15] P. K. Katiyar, R. Maurya, et P. K. Singh, « Corrosion behavior of plain carbon steels under different heat treatment conditions in freely aerated 3.5% NaCl solution », *Int. J. Sustain. Build. Technol. Urban Dev.*, vol. 13, nº 1, p. 44-68, mars 2022, doi: 10.22712/SUSB.20220005.

[16] M. V. Moraschini, S. S. M. Tavares, R. C. P. Loureiro, H. F. G. De Abreu, A. R. Pimenta, et G. Perez, « Effect of Solution Temperature on the Microstructure of 18%Ni Maraging Steel Modified With Nb—X-Ray Diffraction and Electron Backscattered Scanning Diffraction (EBSD) Analyzes », *X-Ray Spectrom.*, vol. 54, nº 5, p. 547-555, sept. 2025, doi: 10.1002/xrs.3491.

[17] W. Zheng, J. Zhu, et W. Yuan, « Tempering stress relaxation behavior and microstructure evolution of 300 M steel », *Mater. Charact.*, vol. 197, p. 112688, mars 2023, doi: 10.1016/j.matchar.2023.112688.

[18] O. Haiko *et al.*, « The Effect of Tempering on the Microstructure and Mechanical Properties of a Novel 0.4C Press-Hardening Steel », *Appl. Sci.*, vol. 9, nº 20, p. 4231, oct. 2019, doi: 10.3390/app9204231.

[19] S. Takebayashi, T. Kunieda, N. Yoshinaga, K. Ushioda, et S. Ogata, « Comparison of the Dislocation Density in Martensitic Steels Evaluated by Some X-ray Diffraction Methods », *ISIJ Int.*, vol. 50, nº 6, p. 875-882, 2010, doi: 10.2355/isijinternational.50.875.

[20] A. Peter, J. Mutua, J. Obiko, et J. Ngoret, « A Comparative Study on the Effect of GMAW Welding Current on the Performance of API 5L GrB Pipeline Steel Welds for Oil and Gas Industrial Applications », *J. Pipeline Sci. Eng.*, p. 100360, Sept. 2025, doi: 10.1016/j.jpse.2025.100360.

[21] Clara. Escrivà-Cerdán, S. W. Ooi, G. R. Joshi, R. Morana, H. K. D. H. Bhadeshia, et Robert. Akid, « Effect of tempering heat treatment on the CO2 corrosion resistance of quench-hardened Cr-Mo

low-alloy steels for oil and gas applications », *Corros. Sci.*, vol. 154, p. 36-48, juill. 2019, doi: 10.1016/j.corsci.2019.03.036.